Understanding rapid changes in phase partitioning in an Arctic stratiform mixed-phase cloud

Heike Kalesse[1], Gijs de Boer[2,3], Amy Solomon[2,3], Mariko Oue[4], Maike Ahlgrimm[5], Damao Zhang[6], Matthew D. Shupe[2,3], Edward Luke[7], Alain Protat[8]

[1] Leibniz Institute for Tropospheric Research, Leipzig, Germany (kalesse@tropos.de)
[2] Cooperative Institute for Research in Environmental Sciences, The University of Colorado, Boulder, CO, USA
[3] NOAA Earth System Research Laboratory, Boulder, CO, USA
[4] School of Marine and Atmospheric Sciences, Stony Brook University, Stony Brook, NY, USA
[5] European Centre for Medium-Range Weather Forecasts (ECMWF), Reading, UK
[6] University of Wyoming, Dep. of Atmospheric Science, WY, USA
[7] Brookhaven National Laboratory, Upton, NY, USA
[8] Bureau of Meteorology, Melbourne, Australia

Motivation

Understanding phase transitions in mixed-phase clouds consisting of liquid droplets and ice particles is of great importance because hydrometeor phase controls the lifetime and the radiative effects of clouds. In high latitudes, these cloud radiative effects have a crucial impact on the surface energy budget and thus on the evolution of land- and ocean-based ice cover.

For a springtime low-level mixed-phase stratiform cloud case at Barrow, Alaska, observed on 11-12 March, 2013, a sophisticated combination of instruments and retrieval methods is combined with multiple modeling perspectives to determine key processes that control transitions in cloud phase partitioning. The interplay of local cloud-scale vs. large-scale processes is considered.

Observations

Instrument	Specifications	Observed/derived quantities
Weather station sensors		T, p, RH, horizontal wind
Radiosondes	every 6-12 hrs	T, p, RH, T_d, Q_v, horizontal wind
Ka-band ARM radar (KAZR)	35 GHz	Cloud top height, IWC, D_{ge}, N_{ice}, W,ε
High Spectral Resolution Lidar (HSRL)	532 nm	Cloud base, cloud phase, D_{ge}, LWC, R_{eff}, N_{liq}
Microwave radiometer (MWR)	23.8 GHz and 31.4 GHz	Column-integrated LWP
Polarimetric X-band scanning precip. radar X-SAPR	Dual-polarisation	Horizontal wind profile
TSI 3563 Nephelometer	450 nm, 550 nm, 700 nm	Total aerosol scattering and backscattering
Particle Soot/Absorption Photometer (PSAP)	467 nm, 530 nm, 660 nm	Aerosol absorption
TSI 3010 Condensation Particle Counter (CPC)	10 nm to 3 μm	Aerosol number concentration

Models

❖ WRF V3.5 (Nested Weather Research and Forecasting)
- Resolution: (horizontal: 12/3/0.5 km (nested grids), vertical: 20m)
- Boundary conditions: 6-hourly ECMWF 16 km analysis
- Microphysics: Morrison bulk two-moment scheme; combined ice+snow particle number relaxed to 1/L

→ Used to study cloud evolution

❖ ECMWF radiation scheme
- Shortwave (SW) and longwave (LW) calculations using Monte Carlo Independent Pixel Approximation

→ Used to determine radiative impacts of a cirrus and the solar cycle

❖ MACC (Monitoring Atmospheric Composition and Climate)
- Chemical transport model including 12 aerosol species

→ Used to estimate aerosol transport and aerosol properties

❖ HYSPLIT
- Hybrid Single-Particle Lagrangian Integrated Trajectory model

→ Used to estimate air mass origins via back trajectory calculations

Radar and lidar observations

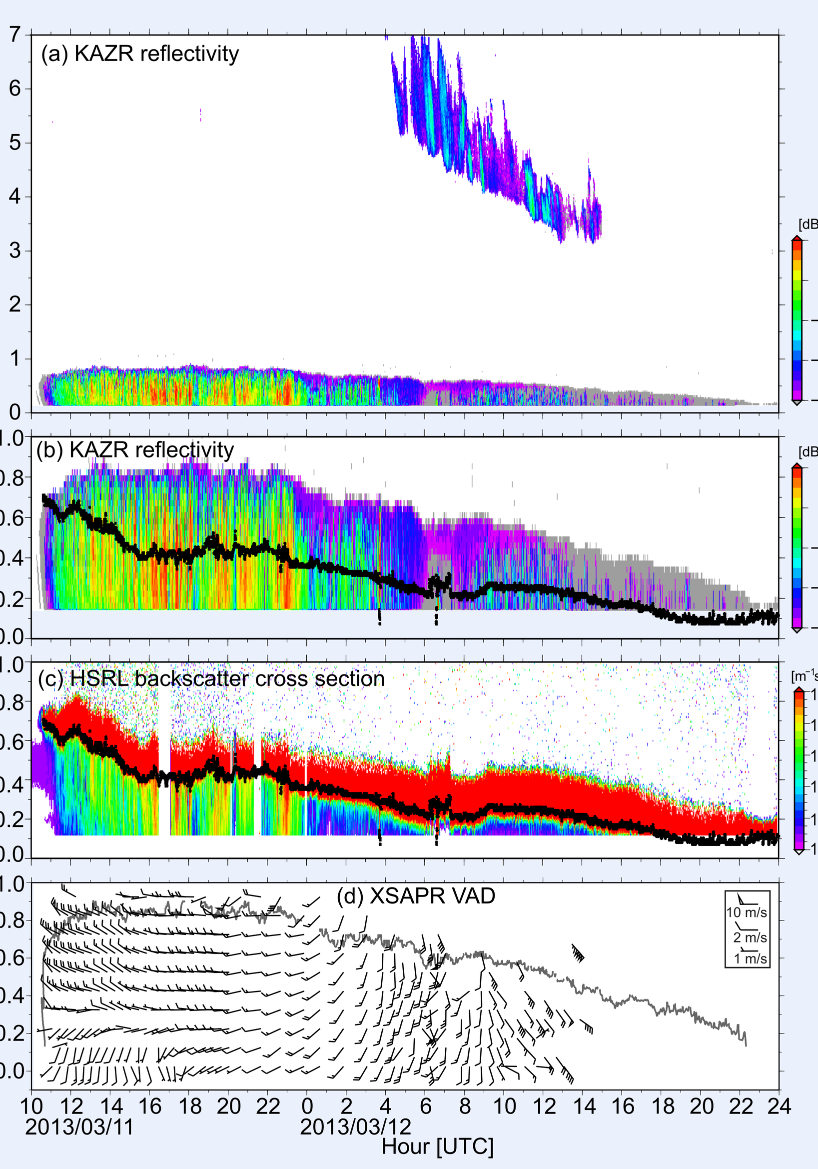

(a) KAZR reflectivity from 0 to 7 km, (b) KAZR reflectivity from 0 to 1 km, (c) HSRL particle backscatter cross section, (d) horizontal winds estimated by the velocity azimuth display (VAD) method using X-SAPR plan position indicator (PPI) scans. Black dots in (b) and (c) represent cloud bases observed by ceilometer. Gray line in (f) represents the -40 dBZ isoline of KAZR reflectivity.

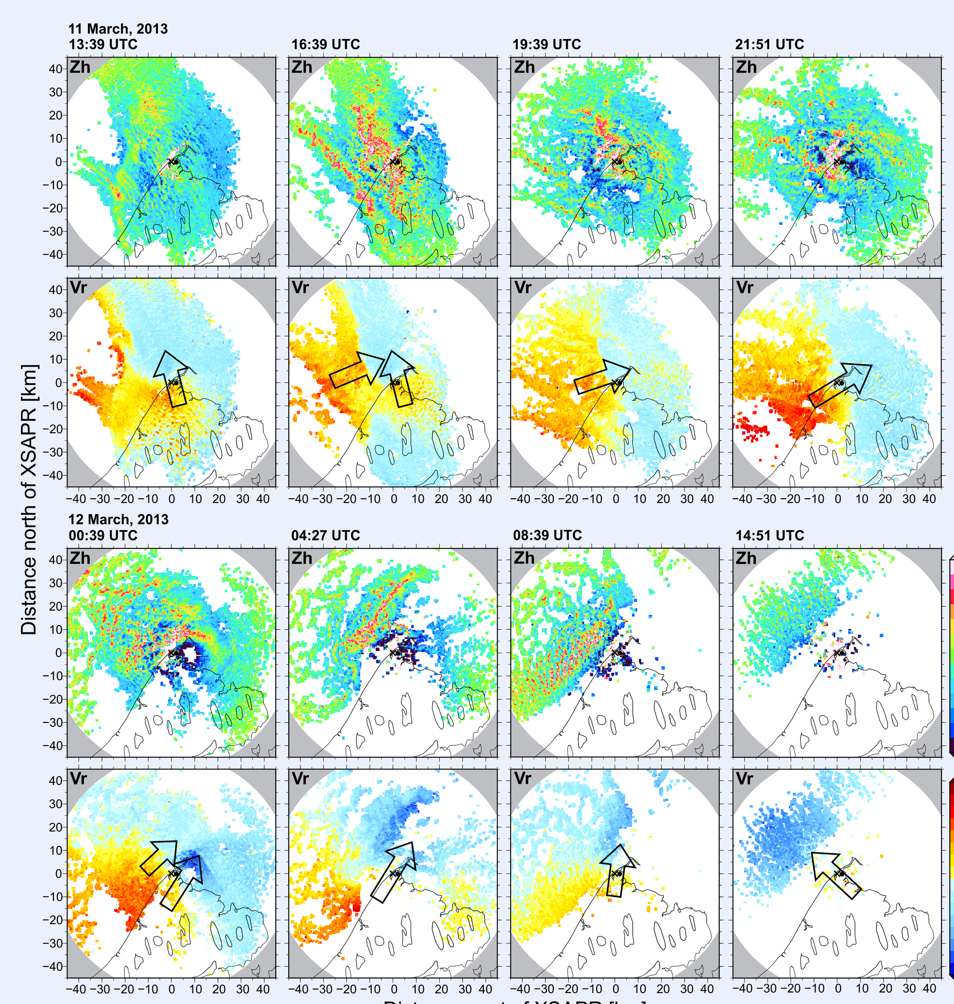

X-SAPR reflectivity (labeled Zh) and Doppler velocity (labeled Vr) from PPI measurements at an elevation angle of 0.5°. Large arrows in the Vr panels represent general wind directions estimated from the Vr measurements.

A low-altitude, mixed-phase stratocumulus is observed for 36 hrs. The passage of a weak warm front with snow showers from the SW is followed by an abrupt decrease in ice as well as a gradual cloud descent and dissipation with winds shifting to S-SE.

Evolution of cloud properties

Microphysical properties

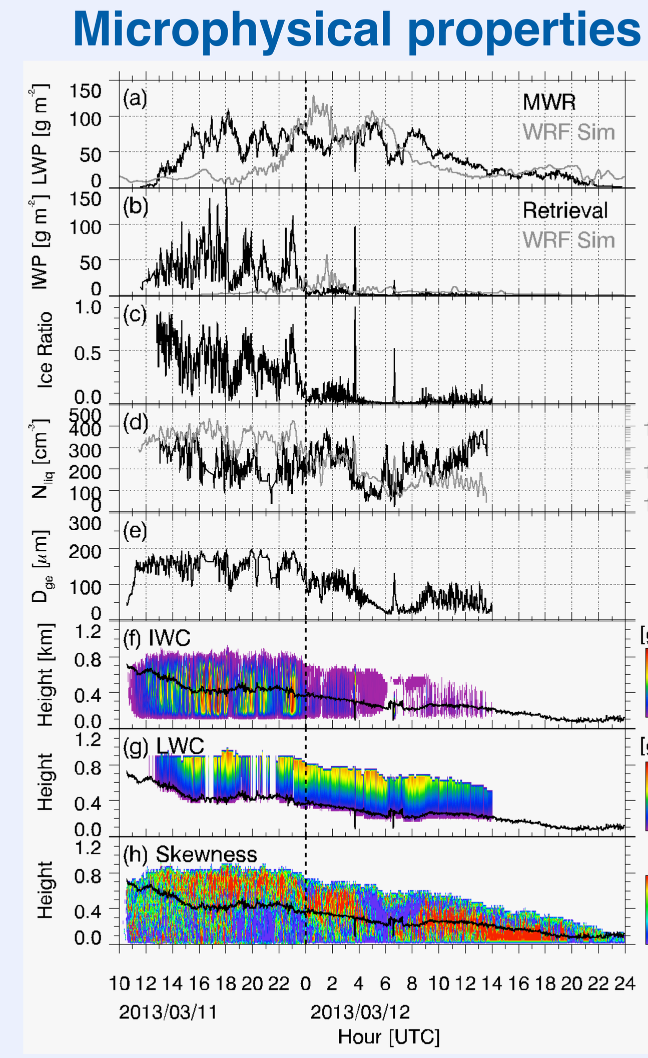

Time series of (a) MWR-derived LWP (black) and WRF simulated LWP (grey), (b) retrieved (black) and WRF simulated (grey) IWP, (c) retrieved ice ratio, (d) retrieved N_{liq} (black) and N_{ice} (grey), (e) retrieved layer-mean D_{ge}, (f) retrieved IWC, (g), retrieved LWC, (h) KAZR Doppler spectra skewness s_D. Black line in (f-h) represents liquid-cloud base observed by ceilometer.

The drop in IWP and N_{ice} is concurrent with the change in surface-coupling and wind direction.

Cloud dynamics

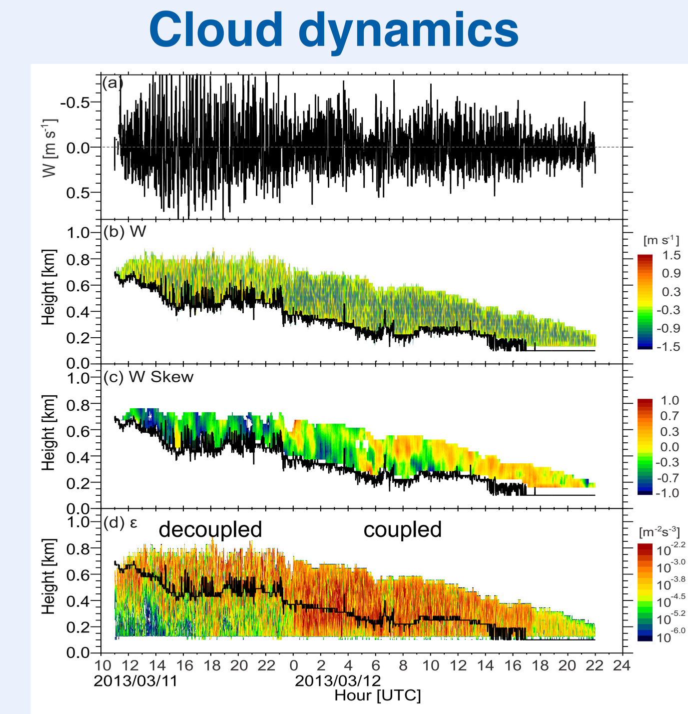

Time series of (a) layer-mean retrieved vertical velocity W, and time-versus-height cross sections of (b) W above liquid-dominated cloud base, (c) skewness of W, and (d) turbulent kinetic energy dissipation rate ε. Black line in (b-d) represents liquid cloud base observed by ceilometer.

WRF results

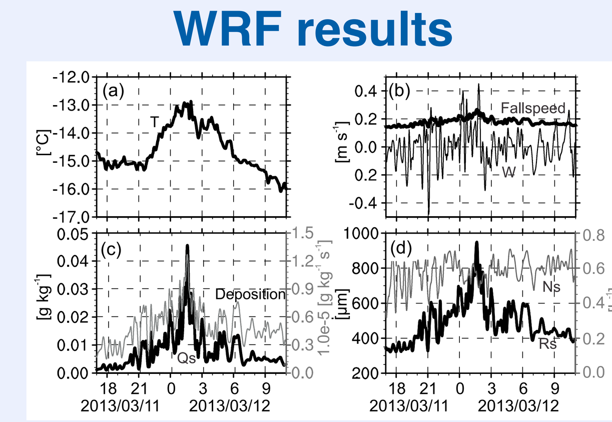

WRF simulation of (a) in-cloud temperature, (b) vertical velocity W (thin line, pos. = upward) and snow fall speed (thick line, pos. = downward), (c) snow mixing ratio (thick black line), snow deposition rate (thin grey line), and (d) snow effective radius (black line), and snow number concentration (grey line).

Atmospheric profiles

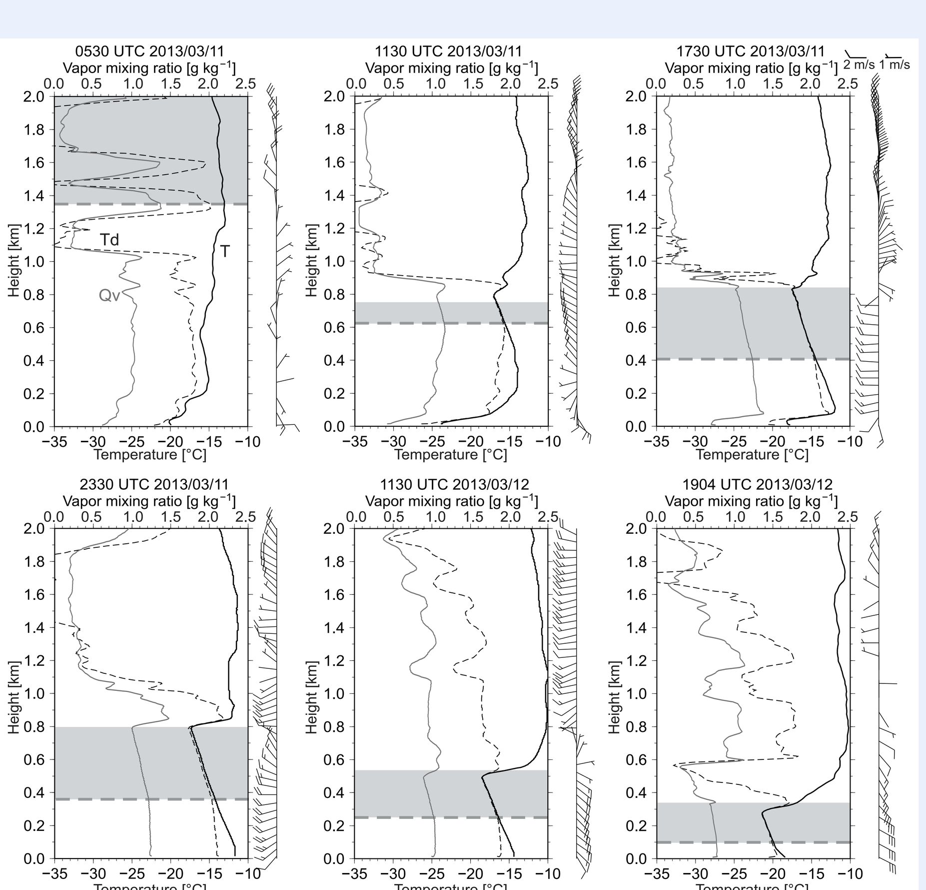

Vertical profiles of temperature (black solid line), dew point temperature (black dashed line), water vapor mixing ratio (grey solid line) and horizontal winds (barbs) observed by radiosoundings at Barrow, Alaska. Horizontal grey dashed lines represent liquid-cloud bases observed by ceilometer. Layers between the liquid-dominated cloud base and highest cloud top estimated from KAZR are represented by grey shading.

Aerosols and advection

Aerosol properties

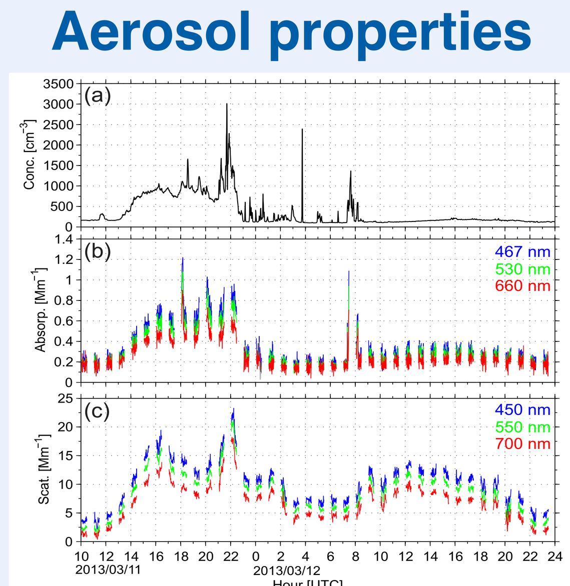

Surface aerosol properties. (a) particle concentration for particles larger than 10 nm (CPC), (b) aerosol absorption (PSAP), and (c) aerosol scattering (nephelometer).

Back trajectories

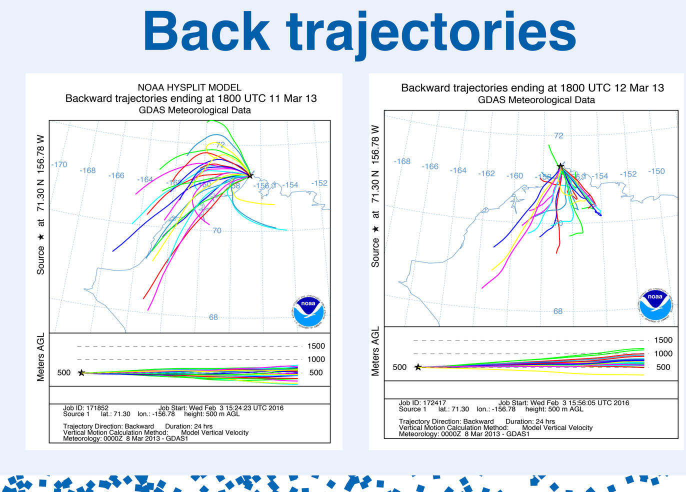

Factors influencing phase transitions

Three main factors were found to contribute to the abrupt change in phase partitioning for this case:

1. Large-scale advection of different air masses with different moisture content and aerosol concentrations played a major role. During the time of highest ice and liquid water contents, the airmass over Barrow had a relatively high aerosol concentration and was supported by moist advection at cloud level from W-SW. This airmass was eventually replaced by a drier southeasterly flow characterized by a reduced aerosol load as well as decreasing cloud and surface temperatures and decreasing water vapor supply.
2. Cloud-scale processes, specifically the cloud-surface thermodynamic coupling state, changed at the time of the airmass transition. Prior to the transition a higher IWP was maintained when the cloud was decoupled from the surface with a relatively dry near-surface layer below the cloud. This structure likely supported sub-cloud sublimation for ice crystals such that IN were not lost to the surface and may have continued to be available to the cloud via IN recycling. After the transition the cloud became coupled to the surface with high levels of moisture extending down to the surface. As a result precipitating ice, including the limited supply of IN, was lost from the cloud system to the surface.
3. WRF simulations suggest that the residence time of ice particles, which is linked to local-scale dynamics, was also important in the change of phase partitioning. Simulated IWP was found to be higher during times of strong updrafts that dominated during the early part of the case. After the transition updrafts weakened and ice crystals fell more quickly from the cloud system.

The radiative shielding of a cirrus on 12 March as well as the influence of the solar cycle were found to be of minor importance for turbulence modulation in the mixed-phase cloud (not shown), and thus likely did not play key roles in the transition.

Observations of aerosol properties, including IN concentrations and vertical profiles of aerosol particle concentrations are ultimately needed to unravel the role of aerosol-cloud interactions in driving transitions in cloud phase partitioning.